mater.scichina.com link.springer.com Published online 15 April 2024 | https://doi.org/10.1007/s40843-024-2914-x

A tough, resilient, and fluorinated solid-electrolyte interphase stabilizing lithium metal in carbonate electrolytes

Jia Kong[1], Tianyi Hou[1], Ting Shi[1], Jianbo Li[1], Xin Deng[1], Dinggen Li[2*], Yunhui Huang[1*] and Henghui Xu[1*]

ABSTRACT **The unstable interface between lithium metal anodes and carbonate-based electrolytes is a key challenge limiting the cycling lifespan of high-energy lithium metal batteries. Here, a resilient artificial solid electrolyte interphase (RASEI) was designed by regulating poly(hexafluorobutyl acrylate) (PHFBA) matrix with the benzene-containing bisphenol A ethoxylate dimethacrylate (BAED) crosslinker to address this issue. The rigid BAED molecule can finely tune the flexible PHFBA matrix, enabling superior resilience from 600% elongation to 90% compression with a high Young's modulus of over 2 MPa. RASEI with these characteristics can accommodate large volume changes of lithium metal and ensure the intimate contact between the lithium metal and the RASEI during battery operation. Consequently, it facilitated homogeneous lithium deposition while mitigating parasitic side reactions. Thanks to the tough and resilient nature of the fluorinated RASEI, the long-term cycling of Li||Li symmetric cells can be achieved for over 500 h at 1 mA cm^{-2} and 1 mAh cm^{-2}. The following post-mortem of cycled Li metal reveals that Li dendrite growth is effectively inhibited. Furthermore, the NCM811 pouch cell with a high cathode loading of 20 mg cm^{-2} exhibits a capacity retention of over 85% after 200 cycles at 1 C.**

Keywords: lithium metal anode, carbonate electrolytes, resilient ASEI, high cathode loading

INTRODUCTION

Lithium metal anode, with a high theoretical specific capacity (3860 mAh g^{-1}) and the lowest redox potential (−3.04 V *vs.* the standard hydrogen electrode), has been considered as the "holy grail" of higher energy density batteries [1,2]. In addition, carbonate electrolytes demonstrate anodic stability at high potentials, which makes them promising candidates for matching with high-voltage cathodes, such as $LiNi_xMn_yCo_{1-x-y}O_2$ and $LiCoO_2$, to achieve higher energy density [3,4]. However, studies have delineated that conventional carbonate electrolytes may not be apt for lithium metal batteries, as they readily undergo reactions with lithium metal anodes, engendering unstable solid-electrolyte interphases (SEIs) [5–7]. Unstable SEIs lead to uncontrolled lithium dendrite growth and limited Coulombic efficiency during repeated plating/stripping processes, which remain key challenges limiting their practical application [8–10].

Up to now, plenty of strategies have been proposed to solve the issue of lithium dendrites, such as electrolyte modification [11–13], separator modification [14–16], and artificial solid electrolyte interfaces (ASEIs) [17–20]. Among these strategies, ASEIs have been extensively explored to enhance the stability of lithium metal anodes. ASEIs can be categorized into inorganic and polymeric interphases [21–23]. Inorganic ASEIs such as LiF [24,25], LiPON [26], Al_2O_3 [27], and others [28–31] exhibit high mechanical strength or excellent ionic conductivity, which can effectively prevent the growth of dendrites. However, their brittle nature makes them prone to fracturing and delamination during lithium stripping/plating, especially under bending and stretching. Loss of contact with the lithium anode leads to uncontrolled dendrite growth and rapid capacity fading. Meanwhile, conventional polymeric ASEIs with narrow elasticity limit typically undergo plastic deformation, which cannot sustain conformal interfacial contact with lithium metal anodes. In contrast, high elastic artificial solid electrolyte interfaces using rubbery polymer matrices exhibit superior flexibility and fracture resistance under large deformation [32–36]. The elastic ASEIs accommodate huge volume changes of lithium metal, ensuring sustained intimate contact with the lithium substrate. Resilient ASEIs (RASEIs) have great potential for lithium metal protection, but there are still few relevant reports.

RASEIs necessitate not only favorable mechanical properties but also specific characteristics including the resistance to electrolyte degradation and facilitation of ion transport at interfaces. A common approach to obtain elastic materials is by introducing an appropriate quantity of multifunctional cross-linking agent into the monomer and achieving cross-linking. By carefully designing the monomers, cross-linking agents, and reaction conditions, it becomes possible to precisely control the physical and chemical properties of the final polymer to better meet diverse application requirements. Extensive investigations have established that fluorinated acrylates exhibit superior electrochemical and thermal stability compared with their non-fluorinated counterparts, thus making them as promising monomers [37–39]. Moreover, the incorporation of fluorine induces the formation of interfacial LiF, which effectively reinforces the integrity of the electrode–electrolyte interface and contributes to extending the battery's lifespan [40,41]. Among various fluorinated acrylates, hexafluorobutyl acrylate offers the advantages of

[1] State Key Laboratory of Material Processing and Die & Mould Technology, School of Materials Science and Engineering, Huazhong University of Science and Technology, Wuhan 430074, China
[2] School of Energy and Power Engineering, Huazhong University of Science and Technology, Wuhan, 430074, China
* Corresponding authors (email: lidinggen@hust.edu.cn (Li D); xuhh@hust.edu.cn (Xu H); huangyh@hust.edu.cn (Huang Y))

being readily available and cost-effective. Furthermore, the inclusion of benzene rings in the cross-linking agent significantly enhances the strength, stiffness, and corrosion resistance of the polymer network.

In this study, we propose a RASEI coating layer on lithium metal (RASEI@Li) to improve the interfacial stability of lithium metal anodes against carbonate-based electrolytes. The RASEI was synthesized by cross-linking hexafluorobutyl acrylate (HFBA) by the bisphenol A ethoxylate dimethacrylate (BAED) *via* an instant photocuring process. The inclusion of a benzene-containing crosslinker regulated the mechanical properties of poly(hexafluorobutyl acrylate) (PHFBA). Remarkably, the RASEI with only 2% BAED content exhibits exceptional resilience, capable of withstanding elongations of up to 600% and compressions of up to 90%, while maintaining a high Young's modulus exceeding 2 MPa. On the one hand, the elasticity of the RASEI coating allows it to stretch and deform alongside the expansion and contraction of lithium metal, thereby minimizing the cracking and delamination. On the other hand, the RASEI coating effectively hinders the dendrite formation by mechanically obstructing the lithium penetration. Thus, the elastic coating with a unique combination of strength, flexibility, and stability, makes it a highly suitable protective layer for high-performance lithium metal anodes.

As a result, the Li||Li symmetric cells incorporating the RASEI@Li demonstrate remarkable cycling stability with a duration exceeding 500 h, under 1 mA cm^{-2}, 1 mAh cm^{-2} in carbonate-based electrolyte. Additionally, the cell with a high-nickel NCM811 cathode (~20 mg cm^{-2}) exhibits an exceptional capacity retention rate of 90% after 190 cycles. Furthermore, a practical pouch cell, coupled with the commercially available high-nickel cathodes and RASEI@Li anode, displays an impressive capacity retention of over 85% over 200 cycles under 1 C discharge conditions.

RESULTS AND DISCUSSION

As shown in Fig. 1a, the RASEI was prepared by cross-linking HFBA and BAED *via* an instant photocuring process, called P(HFBA-BAED). Notably, HFBA is chosen as the primary monomer due to its F-containing functional group, which aids in achieving a more stable electrode-electrolyte interface. In addition, BAED molecules contain benzene rings that significantly enhance the rigidity of the polymer. The precursor solution was coated on the surface of lithium metal using a simple tape-casting technique, and then cured under ultraviolet light to obtain RASEI@Li.

The utilization of UV curing enables the instant reaction, improving production efficiency. The homogeneous precursor solution can be entirely cured by exposing it to a UV lamp for 1 min (Fig. 1b). To verify the cross-linking reactions, Fourier transform infrared (FTIR) spectroscopy was conducted. In the FTIR spectra (Fig. 1c), a clear adsorption peak can be detected at ~1637 cm^{-1} corresponding to the vibration of C=C of the FBA monomer and BAED, while this group cannot be observed in the P(HFBA-BAED). The disappearance of the C=C peak verifies the success of this polymerization reaction. From the X-ray photoelectron spectroscopy (XPS) results (Fig. 1d), a pronounced fluorine (F) signal is observed on RASEI@Li, indicating the presence of the characteristic F element stemming from the P(HFBA-BAED) coating. The emergence of this distinct F signature peak provides the evidence that the P(HFBA-BAED) layer was successfully fabricated onto the lithium metal substrate. Top-view scanning electron microscopy (SEM) image of RASEI@Li is shown in Fig. 1e, where the surface of RASEI@Li is smoother with coating compared with bare Li which has many scratches and pits (Fig. S1). Furthermore, energy-dispersive spectroscopy (EDS) analysis confirmed the uniform distribution of the F element on the lithium metal surface with the elastic coating, providing additional support for the uniformity of the coating (Fig. 1f). Even without adding lithium salts, the fluorine element was still evenly distributed (Fig. S2). Cross-sectional SEM image (Fig. 1g) shows that the elastic coating adhered to the lithium metal with a thickness of <3 μm. In addition, top-view atomic force microscopy (AFM) image provides more detailed evidence for the evenness of lithium metal with elastic coating. As exhibited in Fig. 1h, the surface of RASEI@Li is very smooth with a height variation of about 7.9 nm. Moreover, the possibility of large-scale manufacturing was demonstrated by processing larger areas of lithium ribbons used for the pouch cell assembly. (Fig. 1i).

A coating possessing high mechanical stiffness and good elastic strength can effectively inhibit dendrite growth and adapt to large volume changes of lithium metal to maintain structural integrity [32]. The elastic coating is cross-linked by flexible HFBA and rigid BAED, whereby the mechanical properties of the elastic coating depend on the proportion of the BAED incorporated into the polymer structure. The difference in the physical properties of the elastic coating was characterized by uniaxial tensile and compression testing.

As depicted in Fig. 2a and 2b, the elastic coating with P(HFBA-2%BAED) demonstrates the ability to withstand 90% compression without undergoing the destruction and subsequently recovered its original shape after unloading. However, cross-linked polymers with 5% or 10% BAED are broken and fail to restore their original shape after the compression (Fig. S3). The uniaxial tensile stress–strain curves of the elastic coating with varying BAED contents (Fig. 2c) reveal that as the BAED content increases, their tensile strength gradually increases while causing a gradual decrease in elongation. The rigid planar structure of the benzene ring can improve the rigidity of the polymer chain, enhance the inter-chain interaction force and improve the material strength. The P(HFBA-0%BAED) without the addition of BAED has a linear molecular structure, exhibiting the good molecular chain segment mobility and outstanding tensile properties, and can stretch up to 16 times itself (Fig. S4). The Young's modulus of the P(HFBA-2%BAED) (2.1 MPa) is approximately 52.5 times higher than that of P(HFBA-0%BAED) (0.04 MPa). It is obvious that adding an appropriate amount of BAED can significantly increase the Young's modulus of the P(HFBA-BAED), and it also has an elongation exceeding 600% without fracture (Fig. 2d). However, upon further addition of BAED, the Young's modulus of P(HFBA-5%BAED) (2.74 MPa) is only 1.3 times as high as that of P(HFBA-2%BAED), and the maximum elongation rate decreased to less than 300%. These results indicate that the BAED content does not always positively correlate with the tensile properties of P(HFBA-BAED). Excessive BAED can damage some of its mechanical performance. To sum up, P(HFBA-2%BAED) exhibits significantly superior mechanical behavior, and therefore represents a promising candidate for the elastic coating.

To assess the chemical stability between the elastic coating and

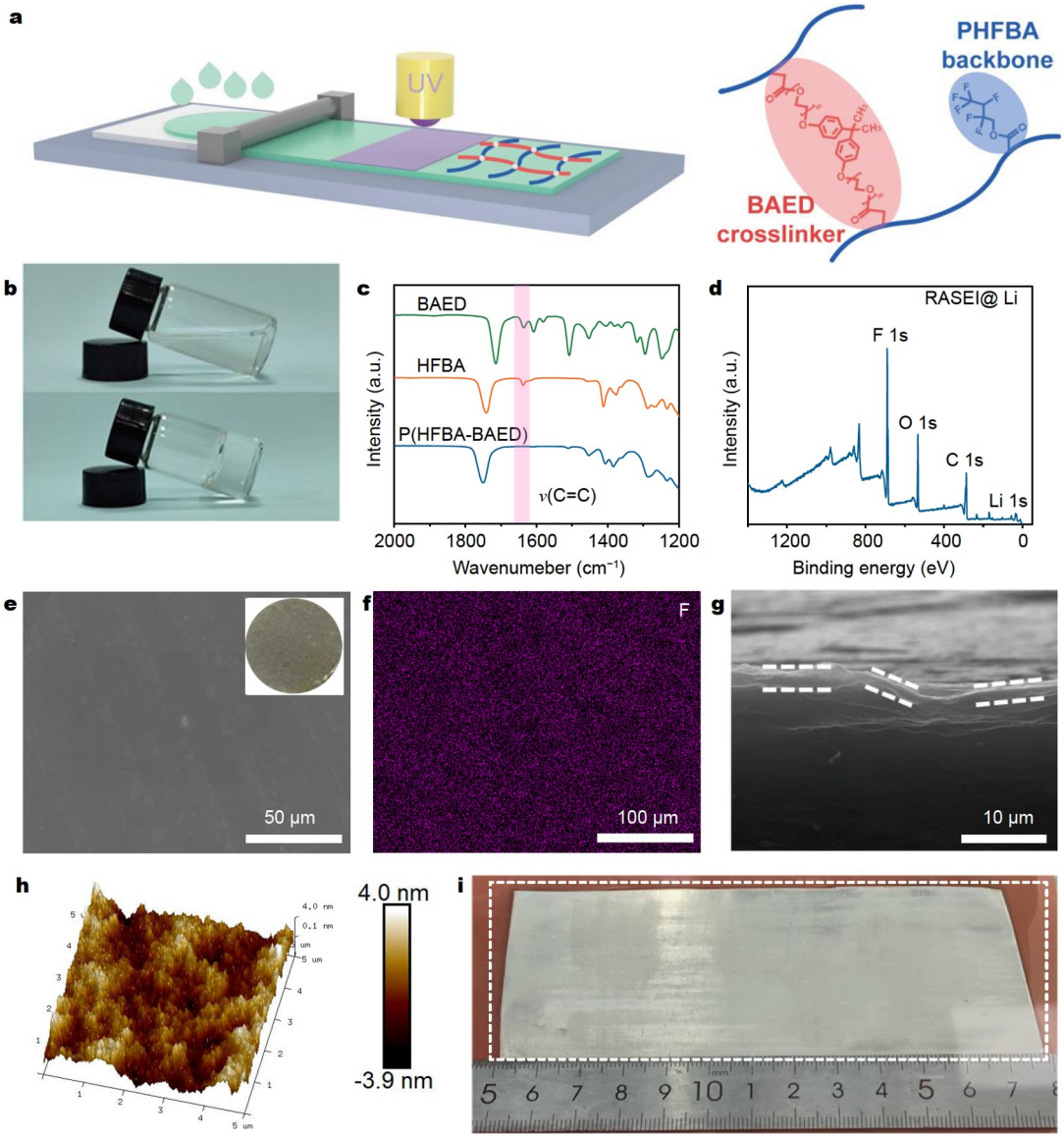

Figure 1 (a) Schematic illustration of the fabrication process of RASEI@Li. (b) Photographs of the P(HFBA-BAED) polymerization process after 1 min of UV curing. (c) FTIR spectra of BAED, HFBA and P(HFBA-BAED). (d) XPS pattern of RASEI@Li. (e) Top-view SEM image of RASEI@Li. The inset in (e) is the photograph of RASEI@Li. (f) EDS elemental mapping image of F for RASEI@Li. (g) Cross-sectional SEM image of RASEI@Li. (h) AFM image of RASEI@Li. (i) Photograph of lithium ribbon with RASEI.

electrolyte, the P(HFBA-BAED) was immersed in a carbonate-based electrolyte, and remained the structural integrity after 30 days (Fig. 2g). The optical photo before P(HFBA-BAED) immersion is shown in Fig. S5. In addition, elastic coating of P(HFBA-BAED) has extremely low electronic conductivity of 1.66×10^{-7} S cm^{-1} (Fig. S6) and good ionic conductivity of 2.52×10^{-6} S cm^{-1} (Fig. S7), which gives the SEI its critical passivating functionality to stabilize the highly reducing anode surface.

To evaluate the effectiveness of RASEI in enhancing the interfacial stability of the lithium metal anode, the cycling performance of the symmetric cells in a carbonate-based electrolyte was investigated. Li||Li symmetric cells employing RASEI@Li anodes with different BAED content of elastic coating were assembled to determine the optimal electrochemical performance configuration. As shown in Fig. 3a, the symmetric cell with an elastic coating of P(HFBA-2%BAED) exhibits excellent cycle stability over 500 h under a high areal capacity of 1 mAh cm^{-2} at a current density of 1 mA cm^{-2}. By contrast, the symmetric cells with bare Li only exhibit significantly reduced cycling life (320 h). Meanwhile, the symmetric cells with the coating of P(HFBA-0%BAED) perform poor cycle stability, and the reason may be that P(HFBA-0%BAED) is too soft and lacks elasticity. In addition, the cycle performance of the symmetric cells with P(HFBA-5/10%BAED) is inferior to those with P(HFBA-2%BAED) (Fig. S8). These findings demonstrate that a coating with a balance of rigidity and flexibility is the most suitable, and P(HFBA-2%BAED) is the optimal formulation thus far. Unless otherwise specified, all ensuing mentions of RASEI will refer to P(HFBA-2%BAED).

The electrochemical impedance spectroscopy (EIS) test result shows that the impedance of Li||Li symmetric cells with RASEI@Li-2% exhibits only a slight increase when compared with bare Li (Fig. S9), suggesting that the coating does not

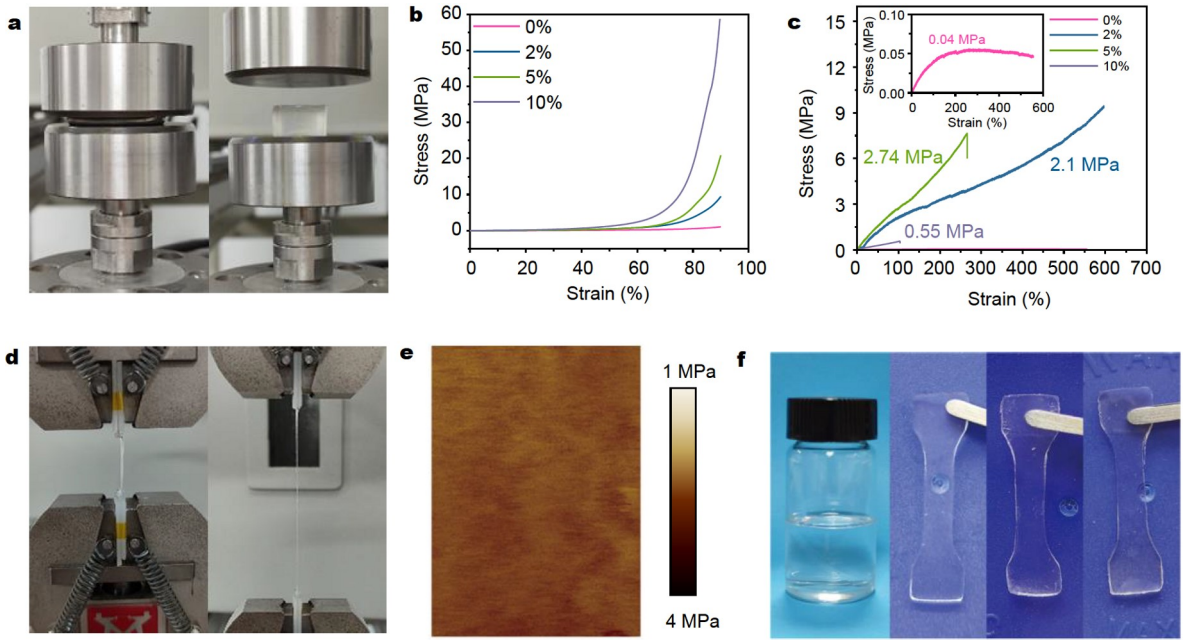

Figure 2 (a) Photographs of P(HFBA-2%BAED) compressed by 90%. (b) Compressive stress–strain curves for P(HFBA-*x*%BAED). (c) The uniaxial stress–strain curves for P(HFBA-*x*%BAED). (d) Uniaxial tensile behavior of P(HFBA-2%BAED). (e) Young's modulus mapping of P(HFBA-2%BAED). (f) Optical images of P(HFBA-BAED) soaked in carbonate-based electrolyte for 10, 20 and 30 days.

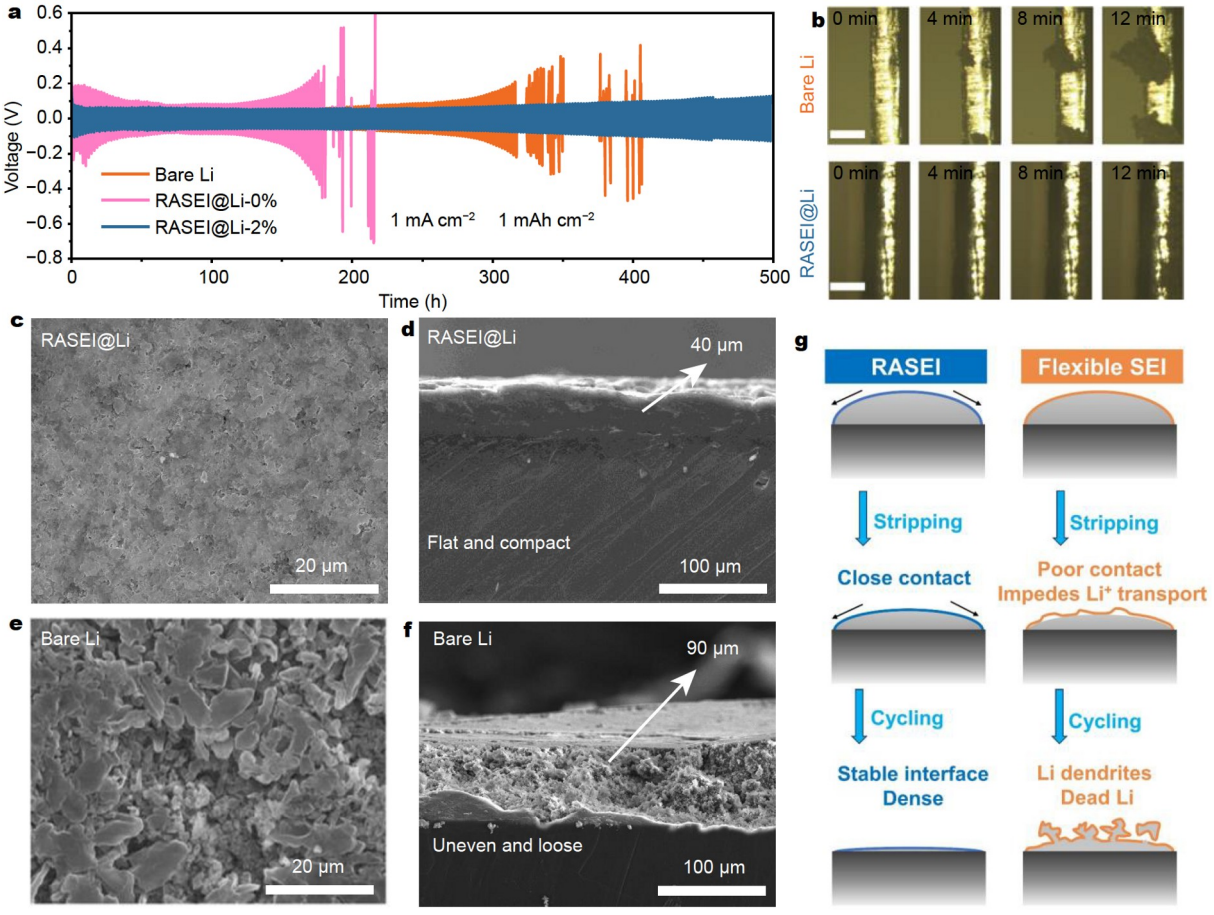

Figure 3 (a) Voltage profiles of bare Li and RASEI@Li-0%/2% anodes in symmetric cell. (b) *In-situ* optical images of Li deposition on bare Li and RASEI@Li in the symmetric cell at different minutes (scale bar, 100 μm). Top surface and cross-sectional SEM images of RASEI@Li (c, d) and bare Li (e, f) after 50 cycles at 1 mAh cm^{-2} and 1 mA cm^{-2}. (g) Li stripping/plating behavior for lithium of RASEI and conventional flexible ASEI.

impede the ion transport at the interface. The Li||Li symmetric cells with RASEI@Li also achieved 1300 h stable cycling under conditions of 0.5 mA $cm^{-2}$of area current density and 1 mAh cm^{-2} of areal capacity, with the overpotential not exceeding 60 mV (Fig. S10). However, for the cells paired with bare Li, the overpotential exceeded 100 mV after 900 h. Moreover, the Li||Li symmetric cells with RASEI@Li also exhibits enhanced cycle performance at an area capacity of up to 4 mAh cm^{-2} compared with the cells with bare Li (Fig. S11). To evaluate the improved stability of the lithium metal interface achieved by RASEI, *in-situ* optical microscopy was used to monitor the Li^+ deposition process. Fig. 3b shows the real-time optical images of the *in-situ* Li deposition on the RASEI@Li and bare Li substrates, recorded at various time intervals (0, 4, 8, and 12 min) at a current density of 2 mA cm^{-2}. The deposition of Li on the surface of bare Li showed non-uniform distribution, accompanied by obvious lithium dendrites, while no visible dendrites were observed in the experiments conducted using RASEI@Li. Due to the excellent mechanical properties of the elastic layer, the growth of Li dendrites on the RASEI@Li surface was effectively suppressed.

To gain further insight into the Li electrodeposition and electrochemical dissolution in bare Li and RASEI@Li, the surface and cross-sectional SEM images of the Li anodes after cycling were acquired. The SEM images revealed that the RASEI@Li surface exhibited a flat and compact morphology (Fig. 3c). Meanwhile, the cross-sectional image confirmed uniform Li deposition (Fig. 3d). By contrast, the surface of cycled bare Li was uneven and cracked, with a loose and porous morphology, indicating serious dendrite growth (Fig. 3e, f). The plating morphology of Li metal on bare Cu and RASEI@Cu electrodes was captured by SEM. As seen in Fig. S12, the Li deposition on RASEI@Cu was compact and continuous after plating with a capacity of 3 mAh cm^{-2}. Quite different from the dense Li layer on the RASEI@Cu electrode, a porous and loose Li deposition occurred on bare Cu at the same current density. As depicted in Fig. S13, the exchange current density of RASEI@Li was twice higher than that of bare Li, which confirmed that RASEI has the potential to enhance Li^+ mobility and rate capability in lithium metal batteries.

To show the advantage of elastic coating, schematics illustrating the structure evolutions of conventional flexible-SEI@Li and RASEI@Li are displayed in Fig. 3g. Due to the good elasticity of ASEI, tight contact between the coating and lithium metal is maintained during lithium plating and stripping. This effectively minimized the side reaction between electrolyte and lithium metal during cycling, enabling uniform Li deposition and suppressing dendrite growth. Conversely, a coating without elasticity will lead to the formation of gaps between the coating and lithium metal during lithium stripping, hindering Li transport and promoting dendrite growth.

In order to demonstrate the potential of the RASEI@Li in lithium metal batteries, the electrochemical performance of Li/NCM811 and Li/LFP cells was investigated. Fig. 4a illustrates the cycling performance of Li/NCM811 cells using bare Li and RASEI@Li at 0.5 C. The cells with RASEI@Li exhibit greatly improved cycling performance (over ~80% capacity retention after 300 cycles), and more stable charge and discharge voltage profile (Fig. S14) than that of cells with bare Li. Moreover, Li/LFP cells with bare Li experience rapid capacity fading, with less than 80% capacity retention after only 220 cycles (Fig. S15a). By contrast, the cells with RASEI@Li demonstrate significantly improved cycling performance, with a capacity retention of ~85% even after 400 cycles. This enhancement is further validated by the galvanostatic charge and discharge curves presented in Fig. S15b and c, which clearly illustrate the substantial capacity fading observed in the bare-Li/LFP cells, whereas the RASEI@Li/LFP cells exhibit minimal capacity changes during cycles. To verify the feasibility of RASEI@Li in practical applications, cells with the NCM811 cathode with a loading capacity of ~20 mg cm^{-2} were assembled for tests. As shown in Fig. 4b, the cells with RASEI@Li delivered a capacity retention of 90% after 190 cycles with a small voltage hysteresis (Fig. S16), while the cells based on bare Li quickly short-circuited after 45 cycles (Fig. 4c). In order to investigate the failure mechanism of the Li/NCM811 cell with bare Li, the disassembly and SEM characterization of the failed cells were conducted after 45 cycles. Fig. S17 demonstrates that the surface of the bare Li electrode exhibits a dendritic structure, which eventually results in the penetration through the separator, ultimately leading to battery failure [42].

Additionally, the surface chemistries of cycled lithium metal anodes were studied *via* X-ray photoelectron spectroscopy (XPS) analysis to further illustrate the advantage of RASEI@Li. In the C 1s spectrum of RASEI@Li after the first cycle (Fig. 4d), the new peak located at ~293.8 eV corresponds to $-CF_3$, which is attributed to elastic coating. In addition, it has a stronger C–C (285.1 eV) peak intensity than bare Li, which probably originates from the HFBA in the protective layer. The above results indicate that the coating was still on the surface of lithium metal after the first cycle. There is a clear peak of CO2− 3 (290.2 eV) in the C 1s spectrum of bare Li, which primarily arises from the decomposition product of solvents through the side reactions. However, the presence of the peak of CO2− 3 is absent on the surface of RASEI@Li, indicating that the RASEI can effectively impede the penetration of the electrolyte and reduce the decomposition of the solvents. To investigate the durability of the coating after extended cycling, Li metal anodes cycled 20 times were also examined. As shown in Fig. 4e, although the peak of CO2− 3 also appears in the C 1s spectrum of RASEI@Li (20%), the peak intensity is much weaker than that of bare Li (25.5%). In the F 1s spectrum of RASEI@Li (Fig. 4f), the prominent CF_3 peak can be observed, as well as corresponding peaks in the C spectrum, indicating that the presence of elastic coating on the lithium metal surface after long-term cycling. Besides, the peak intensity of LiF (684.85 eV) for RASEI@Li is much higher than that of bare Li, which is attributed to the decomposition of HFBA.

Furthermore, a practical pouch cell using commercial high-nickel cathodes and RASEI@Li anodes exhibited an impressive capacity retention of over 85% after 200 cycles under 1/3 C charge and 1C discharge conditions (Fig. 5a, b). Though the pouch cell with bare Li showed a similar capacity at the initial cycles, it experienced a rapid decline after 120 cycles. Compared with other elastic ASEIs, lithium metal batteries equipped with RASEI@Li have excellent cycle performance (Table S1).

To investigate the occurrence of parasitic reactions, particularly gas generation, between the lithium anode and electrolyte, the ultrasonic transmission mapping (UTM) technique was employed [43,44]. The transmitted ultrasonic signal will have an obvious decrease when the ultrasonic wave encounters the gas, which manifests blue color on the distribution map. As shown in

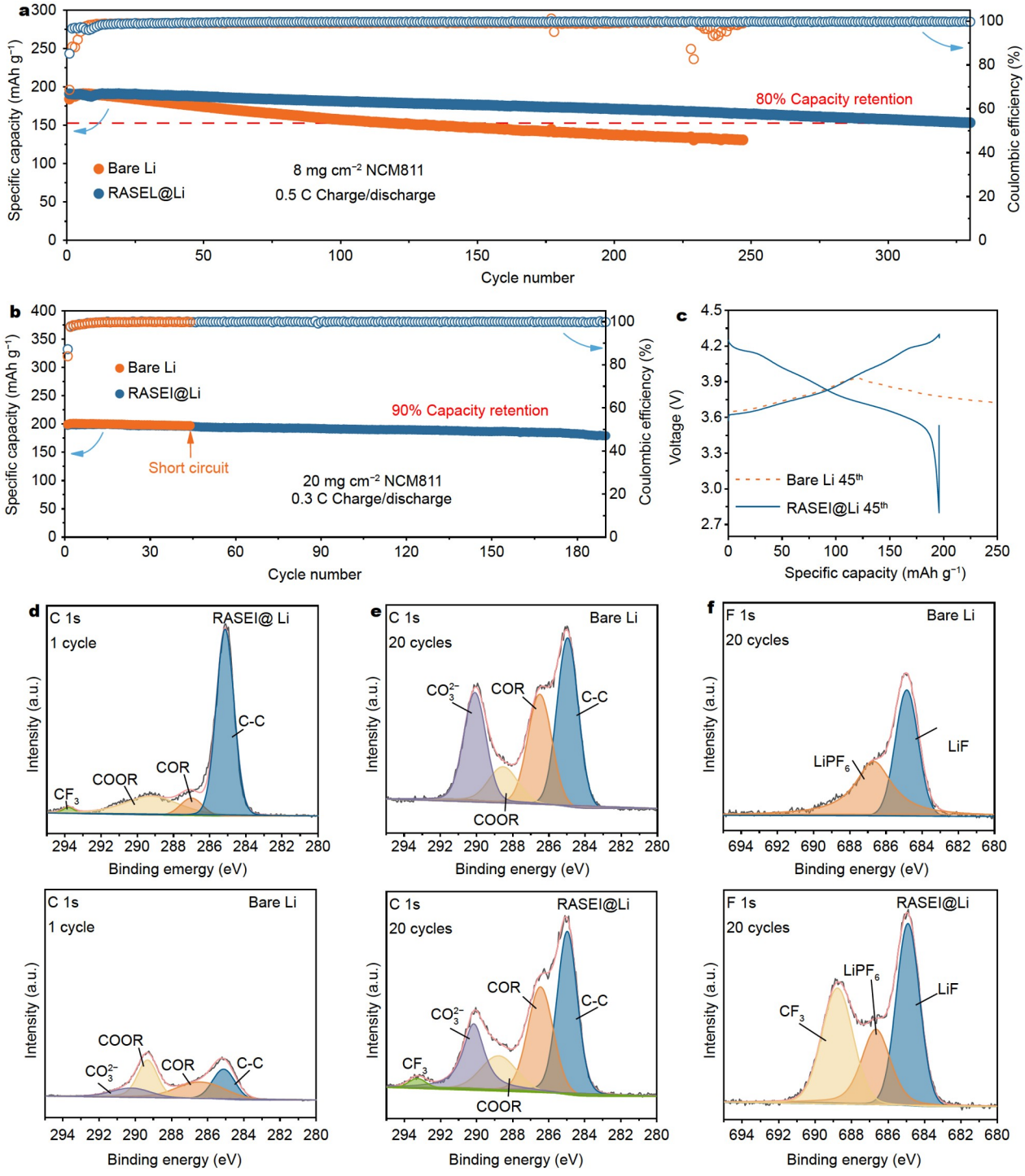

Figure 4 (a) Cycling stability of RASEI@Li/NCM811 and bare Li/NCM811 cells at 0.5 C. (b) Cycling stability of RASEI@Li/NCM811 and bare Li/NCM811 cells at 0.3 C. (c) Voltage profiles of RASEI@Li/NCM811 and bare Li/NCM811 cells at the 45th cycle. (d) C 1s XPS spectra of RASEI@Li and bare Li anodes after 1 cycle. (e) C 1s and (f) F 1s XPS spectra of RASEI@Li and bare Li anodes after 20 cycles.

Fig. 5c, there was no obvious color change in the distribution map, indicating that the pouch with RASEI@Li produced almost no gas in the initial ten cycles. Even after 30 cycles, there were no observable blue signals. By contrast, the map of the pouch cell with bare Li was predominantly covered in blue color after 30 cycles (Fig. 5d), which indicates the occurrence of strong parasitic reactions accompanied by large amounts of gas production. These ultrasound results provide the evidence that the RASEI coating can effectively mitigates side reactions between the electrolyte and Li anode to achieve impressive cycle stability.

CONCLUSIONS

In summary, a resilient artificial solid-state electrolyte interphase (RASEI) coating was developed to enhance the interfacial sta-

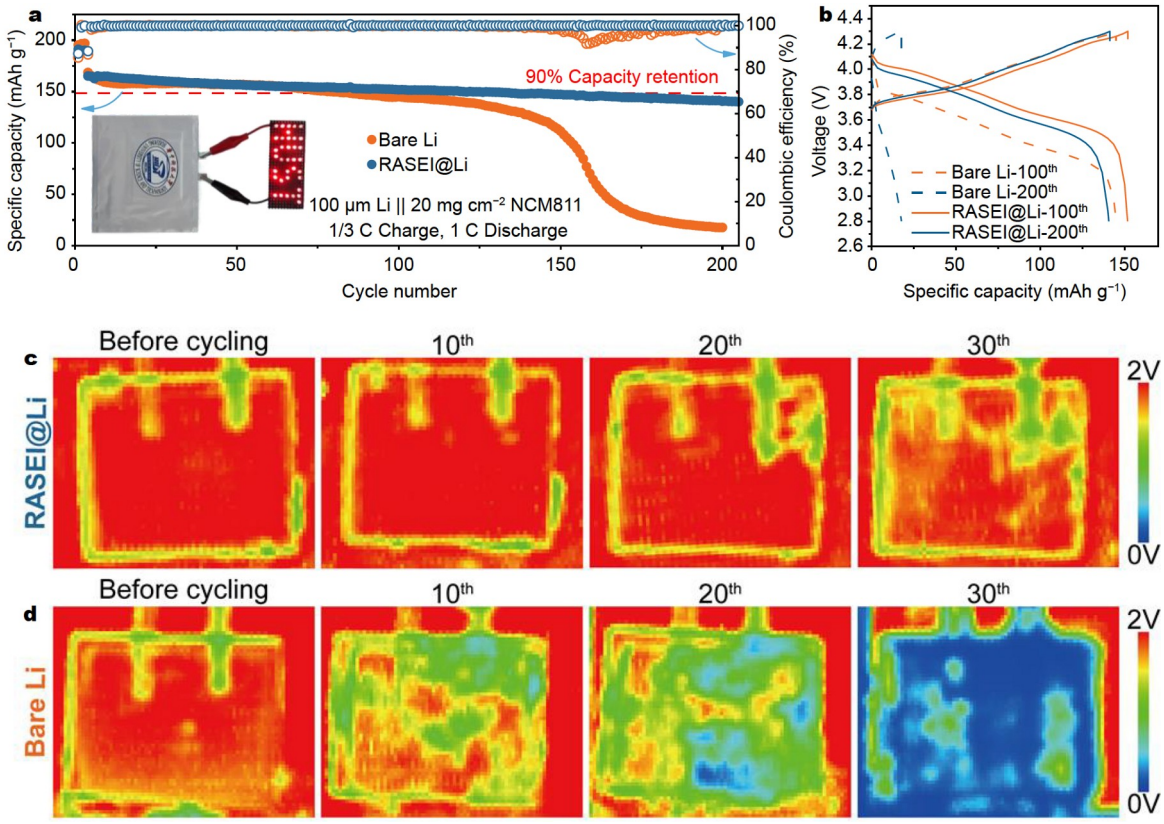

Figure 5 (a) Cycle performances and (b) voltage profiles of RASEI@Li/NCM811 and bare Li/NCM811 cells under 1/3 C charge and 1 C discharge. Ultrasonic transmission mappings of (c) RASEI@Li/NCM811 and (d) bare Li/NCM811 pouch cells.

bility of lithium metal anodes. The mechanical properties of RASEI enable it to withstand the significant volume expansion of lithium metal and maintain conformal interfacial contact during Li plating and stripping processes, thereby ensuring a stable interfacial connection. By acting as a barrier, RASEI effectively hinders the direct contact between the electrolyte and lithium metal anode, leading to a reduction in undesirable side reactions and suppressed growth of lithium dendrites. Moreover, the highly efficient UV curing process offers great potential for large-scale production of RASEI. Through the implementation of RASEI, the Li||Li symmetric cell with the RASEI@Li cycles over 500 h at 1 mA cm^{-2} and 1 mAh cm^{-2} in the carbonate-based electrolyte. Additionally, a practical NCM811/Li pouch cell exhibits a capacity retention of over 85% after 200 cycles under 1/3 C charge and 1 C discharge conditions. Our work highlights the potential value of elastic ASEIs in lithium metal anode protection.

Received 18 January 2024; accepted 1 April 2024; published online 15 April 2024

1 Lin D, Liu Y, Cui Y. Reviving the lithium metal anode for high-energy batteries. Nat Nanotech, 2017, 12: 194–206
2 Xu P, Shuang ZY, Zhao CZ, *et al.* A review of solid-state lithium metal batteries through *in-situ* solidification. Sci China Chem, 2023, 67: 67–86
3 Fang W, Wen Z, Chen L, *et al.* Constructing inorganic-rich solid electrolyte interphase *via* abundant anionic solvation sheath in commercial carbonate electrolytes. Nano Energy, 2022, 104: 107881
4 Yeddala M, Rynearson L, Lucht BL. Modification of carbonate electrolytes for lithium metal electrodes. ACS Energy Lett, 2023, 8: 4782–4793
5 Lu G, Nai J, Luan D, *et al.* Surface engineering toward stable lithium metal anodes. Sci Adv, 2023, 9: eadf1550
6 Xin S, Zhang X, Wang L, *et al.* Roadmap for rechargeable batteries: present and beyond. Sci China Chem, 2023, 67: 13–42
7 Tang W, Ma J, Zhang X, *et al.* Interfacial strategies towards highly stable Li-metal anode of liquid-based Li-metal batteries. Energy Storage Mater, 2024, 64: 103084
8 Chen XR, Zhao BC, Yan C, *et al.* Review on Li deposition in working batteries: from nucleation to early growth. Adv Mater, 2021, 33: 2004128
9 Choudhury S, Mangal R, Agrawal A, *et al.* A highly reversible room-temperature lithium metal battery based on crosslinked hairy nanoparticles. Nat Commun, 2015, 6: 10101
10 Goodenough JB, Kim Y. Challenges for rechargeable Li batteries. Chem Mater, 2009, 22: 587–603
11 Zhu XF, Li X, Liang TQ, *et al.* Electrolyte perspective on stabilizing $LiNi_{0.8}Co_{0.1}Mn_{0.1}O_2$ cathode for lithium-ion batteries. Rare Met, 2023, 42: 387–398
12 Piao N, Liu S, Zhang B, *et al.* Lithium metal batteries enabled by synergetic additives in commercial carbonate electrolytes. ACS Energy Lett, 2021, 6: 1839–1848
13 Xu X, Yue X, Chen Y, *et al.* Li Plating regulation on fast-charging graphite anodes by a triglyme-$LiNO_3$ synergistic electrolyte additive. Angew Chem Int Ed, 2023, 62: e202306963
14 Wu Q, Li L, Zheng Y, *et al.* Achieving physical blocking and chemical electrocatalysis of polysulfides by using a separator coating layer in lithium–sulfur batteries. Sci China Mater, 2024, 67: 107–115
15 Song YH, Wu KJ, Zhang TW, *et al.* A nacre-inspired separator coating for impact-tolerant lithium batteries. Adv Mater, 2019, 31: 1905711
16 Huang X, He R, Li M, *et al.* Functionalized separator for next-generation batteries. Mater Today, 2020, 41: 143–155

17 Yang QY, Yu Z, Li Y, *et al.* Understanding and modifications on lithium deposition in lithium metal batteries. Rare Met, 2022, 41: 2800–2818
18 Zhang C, Yang Y, Sun Y, *et al.* 2D sp^2-carbon-linked covalent organic frameworks as artificial SEI film for dendrite-free lithium metal batteries. Sci China Mater, 2023, 66: 2591–2600
19 Wu J, Rao Z, Liu X, *et al.* Polycationic polymer layer for air-stable and dendrite-free Li metal anodes in carbonate electrolytes. Adv Mater, 2021, 33: e2007428
20 Liu K, Pei A, Lee HR, *et al.* Lithium metal anodes with an adaptive "solid-liquid" interfacial protective layer. J Am Chem Soc, 2017, 139: 4815–4820
21 Yu Z, Cui Y, Bao Z. Design principles of artificial solid electrolyte interphases for lithium-metal anodes. Cell Rep Phys Sci, 2020, 1: 100119
22 Jagger B, Pasta M. Solid electrolyte interphases in lithium metal batteries. Joule, 2023, 7: 2228–2244
23 Han Z, Zhang C, Lin Q, *et al.* A protective layer for lithium metal anode: why and how. Small Methods, 2021, 5: e2001035
24 Chen L, Chen KS, Chen X, *et al.* Novel ALD chemistry enabled low-temperature synthesis of lithium fluoride coatings for durable lithium anodes. ACS Appl Mater Interfaces, 2018, 10: 26972–26981
25 Tan J, Matz J, Dong P, *et al.* A growing appreciation for the role of LiF in the solid electrolyte interphase. Adv Energy Mater, 2021, 11: 2100046
26 Wang W, Yue X, Meng J, *et al.* Lithium phosphorus oxynitride as an efficient protective layer on lithium metal anodes for advanced lithium-sulfur batteries. Energy Storage Mater, 2019, 18: 414–422
27 Chen L, Connell JG, Nie A, *et al.* Lithium metal protected by atomic layer deposition metal oxide for high performance anodes. J Mater Chem A, 2017, 5: 12297–12309
28 Yan C, Cheng XB, Yao YX, *et al.* An armored mixed conductor interphase on a dendrite-free lithium-metal anode. Adv Mater, 2018, 30: e1804461
29 Guo JC, Tan SJ, Zhang CH, *et al.* A self-reconfigured, dual-layered artificial interphase toward high-current-density quasi-solid-state lithium metal batteries. Adv Mater, 2023, 35: e2300350
30 Alaboina PK, Rodrigues S, Rottmayer M, *et al. In situ* dendrite suppression study of nanolayer encapsulated Li metal enabled by zirconia atomic layer deposition. ACS Appl Mater Interfaces, 2018, 10: 32801–32808
31 Pathak R, Chen K, Gurung A, *et al.* Fluorinated hybrid solid-electrolyte-interphase for dendrite-free lithium deposition. Nat Commun, 2020, 11: 93
32 Gu M, Rao AM, Zhou J, *et al. In situ* formed uniform and elastic SEI for high-performance batteries. Energy Environ Sci, 2023, 16: 1166–1175
33 Chen C, Zhang J, Hu B, *et al.* Dynamic gel as artificial interphase layer for ultrahigh-rate and large-capacity lithium metal anode. Nat Commun, 2023, 14: 4018
34 Tamate R, Peng Y, Kamiyama Y, *et al.* Extremely tough, stretchable gel electrolytes with strong interpolymer hydrogen bonding prepared using concentrated electrolytes to stabilize lithium-metal anodes. Adv Mater, 2023, 35: 2211679
35 Li Q, Zeng FL, Guan YP, *et al.* Poly (dimethylsiloxane) modified lithium anode for enhanced performance of lithium-sulfur batteries. Energy Storage Mater, 2018, 13: 151–159
36 Yang N, Cui Y, Su H, *et al.* A chemically bonded ultraconformal layer between the elastic solid electrolyte and lithium anode for high-performance lithium metal batteries. Angew Chem Int Ed, 2023, 62: e202304339
37 Han J, Lee MJ, Min JH, *et al.* Fluorine-containing phase-separated polymer electrolytes enabling high-energy solid-state lithium metal batteries. Adv Funct Mater, 2024, 34: 2310801
38 Huang J, Shen Z, Robertson SJ, *et al.* Fluorine grafted gel polymer electrolyte by *in situ* construction for high-voltage lithium metal batteries. Chem Eng J, 2023, 475: 145802
39 Yang B, Pan Y, Li T, *et al.* High-safety lithium metal pouch cells for extreme abuse conditions by implementing flame-retardant perfluorinated gel polymer electrolytes. Energy Storage Mater, 2024, 65: 103124
40 Xue T, Qian J, Guo X, *et al.* Tailoring fluorine-rich solid electrolyte interphase to boost high efficiency and long cycling stability of lithium metal batteries. Sci China Chem, 2023, 66: 2121–2129
41 Wang Y, Wu Z, Azad FM, *et al.* Fluorination in advanced battery design. Nat Rev Mater, 2024, 9: 119–133
42 Liang J, Chen Q, Liao X, *et al.* A nano-shield design for separators to resist dendrite formation in lithium-metal batteries. Angew Chem Int Ed, 2020, 59: 6561–6566
43 Deng Z, Huang Z, Shen Y, *et al.* Ultrasonic scanning to observe wetting and "unwetting" in Li-ion pouch cells. Joule, 2020, 4: 2017–2029
44 Deng Z, Lin X, Huang Z, *et al.* Recent progress on advanced imaging techniques for lithium-ion batteries. Adv Energy Mater, 2020, 11: 2000806

Acknowledgements This work was supported by National Key R&D Program of China (2023YFB2503801), the National Natural Science Foundation of China (Grant Nos. 52302253, and 5202780089), the Key Program of the National Natural Science Foundation of China (Grant No. 52231009), the Fundamental Research Funds for the Central Universities (HUST: 2172020kfyXJJS089), Key R&D Program of Hubei Province (2023BAB028). The authors thank the Analytical and Testing Centre of HUST and the State Key Laboratory of Materials Processing and Die & Mold Technology of HUST for XRD and SEM measurements. The authors thank the Neware Technology Limited for the electrochemical testing. Thanks to eceshi (www.eceshi.com) for FTIR.

Author contributions Kong J and Hou T conceived the project. Kong J designed the experiments and collected all data, Deng X, Li J helped with the characterization and data analysis. Kong J wrote the paper with support from Shi T, Hou T. Li D, Xu H and Huang Y provided critical feedback and helped shape the manuscript.

Conflict of interest The authors declare no conflict of interest.

Supplementary information Experimental details and supporting data are available in the online version of the paper.

Jia Kong is currently a Master degree candidate at the School of Materials Science and Engineering, Huazhong University of Science and Technology. His current research mainly focuses on lithium metal batteries.

Henghui Xu received his PhD at Huazhong University of Science and Technology (HUST) in 2015, followed by a five-year postdoctoral research at The University of Texas at Austin. He is now a Professor of materials science in HUST working on solid-state batteries.

Yunhui Huang received his BS, MS, and PhD degrees from Peking University. From 2002 to 2004, he worked as an associate professor at Fudan University. He then worked with Prof. John B. Goodenough at the University of Texas at Austin for more than three years. In 2008, he became a chair professor of materials science at Huazhong University of Science and Technology. His research group works on rechargeable batteries and electrode materials.

坚韧、弹性的氟化固体电解质界面稳定碳酸酯电解质中的锂金属

孔佳[1], 侯添壹[1], 石婷[1], 李剑波[1], 邓鑫[1], 李顶根[2*], 黄云辉[1*], 许恒辉[1*]

摘要 锂金属负极和碳酸酯类电解液之间不稳定的界面是限制高比能锂金属电池循环寿命的关键挑战. 本文使用含苯环的双酚A乙氧基化物二甲基丙烯酸酯(BAED)交联剂调节聚(丙烯酸六氟丁酯)(PHFBA), 设计了一种弹性人造固体电解质中间相(RASEI)来解决这个问题. 刚性BAED分子可以对柔性PHBA基体进行调控, 实现从600%伸长率到90%压缩率的卓越回弹性, 并具有超过2 MPa的高杨氏模量. RASEI可以适应锂金属较大的体积变化, 并确保电池运行过程中锂金属与RASEI之间的紧密接触, 促进均匀的锂沉积并减少副反应. 因此, 经过RASEI修饰的Li||Li对称电池可以在1 mA cm^{-2}和 1 mAh cm^{-2}下实现超过500小时的长期循环. 对循环后锂金属进行测试分析表明锂枝晶的生长得到了有效的抑制. 此外, 搭配20 mg cm^{-2}高阴极负载的NCM811软包电池在1 C下, 经过200次循环后容量保持率超过85%.